Bull. Mater. Sci., Vol. 34, No. 1, February 2011, pp. 1–9. © Indian Academy of Sciences.

Synthesis, characterization and gas sensing performance of SnO_2 thin films prepared by spray pyrolysis

GANESH E PATIL, D D KAJALE, D N CHAVAN[†], N K PAWAR[††], P T AHIRE, S D SHINDE[#], V B GAIKWAD[#] and G H JAIN[*]

Materials Research Laboratory, Arts, Commerce and Science College, Nandgaon 423 106, India
[†]Department of Chemistry, Arts, Commerce and Science College, Lasalgaon 422 306, India
[††]Department of Physics, Arts, Commerce and Science College, Satana 423 301, India
[#]Materials Research Laboratory, K.T.H.M. College, Nashik 422 005, India

MS received 14 September 2009; revised 11 November 2009

Abstract. **In this work, SnO_2 thin films were deposited onto alumina substrates at 350°C by spray pyrolysis technique. The films were studied after annealing in air at temperatures 550°C, 750°C and 950°C for 30 min. The films were characterized by X-ray diffraction (XRD), scanning electron microscopy (SEM) and optical absorption spectroscopy technique. The grain size was observed to increase with the increase in annealing temperature. Absorbance spectra were taken to examine the optical properties and bandgap energy was observed to decrease with the increase in annealing temperature. These films were tested in various gases at different operating temperatures ranging from 50–450°C. The film showed maximum sensitivity to H_2S gas. The H_2S sensing properties of the SnO_2 films were investigated with different annealing temperatures and H_2S gas concentrations. It was found that the annealing temperature significantly affects the sensitivity of the SnO_2 to the H_2S. The sensitivity was found to be maximum for the film annealed at temperature 950°C at an operating temperature of 100°C. The quick response and fast recovery are the main features of this film. The effect of annealing temperature on the optical, structural, morphological and gas sensing properties of the films were studied and discussed.**

Keywords. **SnO_2 thin films; spray pyrolysis; H_2S gas sensor; sensitivity; selectivity.**

1. Introduction

Since the last decade there has been a great deal of interest in the preparation of inexpensive thin films of SnO_2. This is because tin dioxide based thin films with large bandgap ($E_g > 3$ eV) *n*-type semiconductors are attractive from the scientific and technological point of view (Chopra *et al* 1983). Several potential applications have been reported previously, such as a transparent conductive electrode for solar cells (Aoki and Sasakura 1970; Mohammadi *et al* 2005), a gas sensing material for gas sensors devices (Keshavraja *et al* 1995), transparent conducting electrodes (Fukano and Motohiro 2004), photochemical and photoconductive devices in liquid crystal display (Betz *et al* 2006), gas discharge display, lithium-ion batteries, etc.

A variety of techniques have been used to deposit tin oxide (SnO_2) thin films. These include spray pyrolysis (Paraguay *et al* 1999), ultrasonic spray pyrolysis (Blandenet *et al* 1981), chemical vapour deposition (Baranauskas *et al* 2002), activated reactive evaporation (Randhawa *et al* 1981), ion-beam assisted deposition, sputtering (Vossen and Poliniak 1972), and sol–gel (Chatelon *et al* 1994; Oreal *et al* 1994) methods. Among these techniques, spray pyrolysis has proved to be simple, reproducible and inexpensive, as well as suitable for large area applications. Besides the simple experimental arrangement, high growth rate and mass production capability for large area coatings make them useful for industrial as well as solar cell applications. In addition, spray pyrolysis opens up the possibility to control the film morphology and particle size in the nm range. As demonstrated (Patil 1999), spray pyrolysis is a versatile technique for deposition of metal oxides. Up to now, many researchers have prepared SnO_2 using chemical spray pyrolysis. For example, it has grown tin dioxide thin films (Korotcenkov *et al* 2005) by spray pyrolysis on Si substrates and reported evolution of the crystallographic orientation of the films with variation of the pyrolysis temperature. It is reported (DiBattista *et al* 2000) that the crystallite sizes in the films could be controlled over a nm range by varying the film thickness, deposition method and post-deposition annealing temperature.

However, metal oxides have been used for nearly four decades for gas sensing applications (Khadayate *et al* 2007) and their gas sensing ability was first discovered by Seiyama *et al* (1962) who reported that ZnO thin films exhibit changes in their electrical conductivity with small amount of reducing

[*]Author for correspondence (gotanjain@rediffmail.com)

gases and the same year by Taguchi (1962) who reported that partially sintered SnO_2 pellets respond similarly. These were the beginning for what has been a rapid gas sensor development phase. Also some recent studies on the sensing properties of pure nanocrystalline SnO_2 thin films toward H_2S (Vuong *et al* 2005) and H_2 (Korotcenkov *et al* 2003) seemed to contradict the general trend that higher sensitivity is to be expected for smaller crystals, and it was, therefore, concluded that small size of crystals was an essential but not sufficient condition for the achievement of maximum gas sensitivity and fast response. It is also reported that (Liu *et al* 2009) the sensitive properties of SnO_2 nanocrystals toward low concentrations of H_2S gas in air (0·7–100 ppm) at 25–250°C which showed maximum response at about 150°C, and the response as a function of H_2S concentration. Therefore, our objective in this work was to prepare SnO_2 thin films by the spray pyrolysis method and to investigate the influence of annealing on the properties. Also this paper demonstrates the H_2S sensing properties of SnO_2 thin films. The results of these studies are presented here.

2. Experimental

2.1 *Preparation of spraying solutions*

All the chemicals used in the work were of analytical grade. Tin (II) dichloride dihydrate ($SnCl_2{\cdot}2H_2O$) (99·8 %, Aldrich) was dissolved in a wide variety of solvents. The most common solvents seemed to be water and alcohols. Alcoholic solvents were the most preferred because of their low surface tension and viscosity facilitates the formation of small spray droplets while its low boiling point enables it to be efficiently removed from the deposition chamber in the vapour phase (Chopra *et al* 1983). In the present study, $SnCl_2{\cdot}2H_2O$ (0·075 M) was dissolved in de-ionized water to the required concentration. A few drops of HCl were added to increase clarity of the solution.

2.2 *Details of spray pyrolysis system*

The schematic experimental set up of the spray pyrolysis system which is built in our lab is shown in figure 1. It consists of spray gun with nozzle, substrate heater, automatic temperature control unit, air compressor, pressure regulator, thermocouple, stepper motor with controller and power supply. The heater is a stainless steel block furnace electrically controlled by an automatic temperature controller unit to attain the required substrate temperature to an accuracy of $\pm$ 2°C. The resulting temperature on the surface of the substrate is measured with a chromel–alumel thermocouple. Hazardous fumes evolved during thermal decomposition of the precursor are driven out through an exhaust system attached to the spray pyrolysis unit. The spray nozzle is made up of borocil glass having different bore diameters (viz. 0·1 mm, 0·3 mm, 0·5 mm). Due to air pressure of the carrier gas, a vacuum is created at the tip of the nozzle to suck the solution from the tube after which the spray starts. The spray nozzle is fixed at an appropriate distance from the substrate. The precursor solution was sprayed on to the substrate in air as small drops and around a high temperature zone where thermal decomposition and possible reaction between solutions occur, through compressed air, which is used as carrier gas with a flow rate controlled through air compressor regulator.

To achieve uniform deposition, the moving arrangement has been used. For this, substrate is kept stationary, while the nozzle is free for to and fro motion with mechanical moving

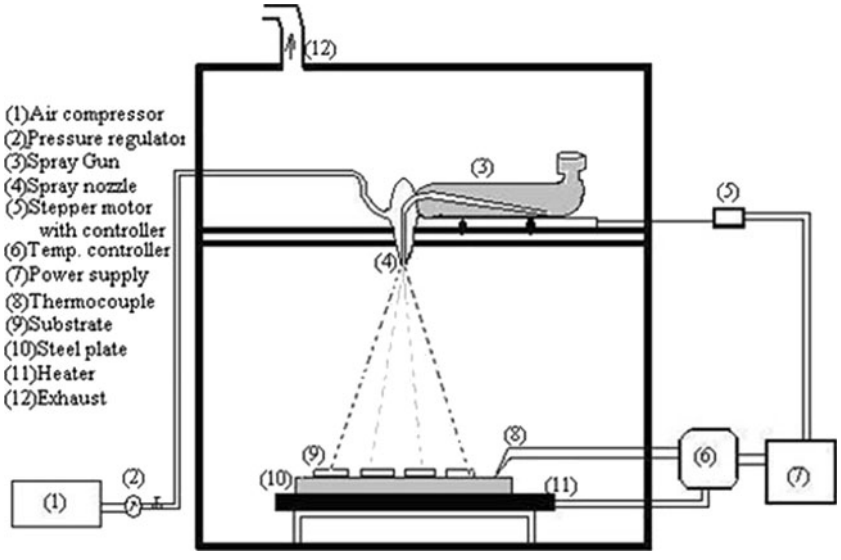

Figure 1. Schematic representation of the spray system.

arrangement as stepper motor has been advantageous, so we do not have to spend energy moving the table with the hot plate and all electrical connections. The nozzle system is very lightweight with easy slider trolley attached. The spraying system and heater are kept inside a metallic chamber of size $60 \times 60 \times 60$ cm^3. The inner surface of the box is painted by epoxy liquid, to reduce heat loss through the surface.

2.3 *Kinetics in thin film deposition*

The deposition process needs fine droplets to react on the heated substrate, owing to the pyrolytic decomposition of the solution. The hot substrate provides the thermal energy for the thermal decomposition and subsequent recombination of the constituent species. In many cases large droplets of the solution do not vaporize before reacting to deposit on the substrate. They hit the surface and form a powdery deposit. If it strikes at a high enough velocity, the droplet will splatter and form a dispersed powdery layer. As mentioned above, the droplet cannot be completely vaporized before it hits the surface and for this reason, film growth cannot occur. Sears and Gee (1998) investigated the mechanism of SnO_2 film growth. The influence of forces which determine both the trajectory of the droplets and evaporation were examined and a film growth model was proposed. Figure 2 shows the types of trajectories that are expected to occur in the spraying of a solution on hot glass substrate.

It is reported that the behaviour of precursor drops undergo three major steps during the course of spray pyrolysis: (i) drop size shrinkage due to evaporation, (ii) conversion of precursor into oxides, and (iii) solid particle formation. The particle formation may involve two mechanisms: intraparticle reaction (conventional one-particle-per-drop mechanism) and gas-to-particle conversion (Kodas and Hampden-Smith 1999). In the one-particle-per-drop mechanism, each droplet is regarded as a micro reactor and converts into one solid particle when it travels towards substrate. In contrast, gas-to-particle conversion occurs when the precursor is volatile and is transported across the particle–gas interface (Gurav *et al* 1995; Kodas and Hampden-Smith 1999). He also measured precursor drop size precisely. He found that bimodal particle size distributions were produced, suggesting that both one-particle-per-drop and gas-to-particle conversion mechanisms were involved in spray pyrolysis.

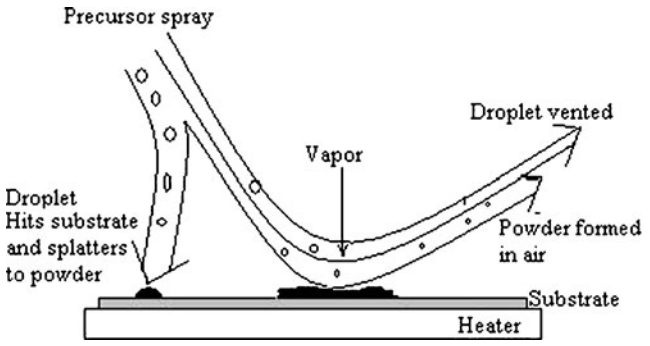

Figure 2. Kinetics in thin film deposition.

The phenomenon for the preparation of a metal oxide thin film depends on surface hydrolysis of metal chloride on a heated substrate surface in accordance with the equation (Hartnagel 1995),

$$XCl_m + nH_2O \rightarrow XO_n + m\text{HCl}, \quad (1)$$

where X is the metal such as Sn, Zn, Cu etc of the oxide films.

2.4 *Preparation of thin films*

As prepared precursor solution of $SnCl_2{\cdot}2H_2O$ (0·075 M) was sprayed, through a glass nozzle of 0·1 mm bore diameter, over a hot glass substrate by means of air as a carrier gas so as to reach a substrate in the form of very fine droplets. Prior to deposition the glass substrate ($75 \times 25 \times 1{\cdot}2$ mm), was cleaned by an ultrasonic cleaner to make the surface hydrophilic. The glass substrate was kept at a temperature of 350°C. The spray rate of 5 mL/min was maintained using air compressor regulator. The distance between spray nozzle and substrate was fixed at 25 cm. After deposition process was completed, the films were kept on the heater at a deposition temperature for 30 min in order to provide sufficient time and temperature for recrystallization. This resulted in formation of well adherent, whitish coloured and uniform SnO_2 thin films. The SnO_2 formulation can be represented as:

$$SnCl_2 + 2H_2O \rightarrow SnO_2 + 2H_2 \uparrow + Cl_2 \uparrow . \quad (2)$$

In the present study, all the spray parameters were kept constant as shown in table 1. As-prepared SnO_2 thin films were used for further characterization by different annealing temperatures for 30 min (table 1).

2.5 *Characterization*

The structural, morphological and optical properties have been studied. The crystalline structure of the thin films, obtained at different annealing temperatures were examined by X-ray diffractometer (Miniflex Model, Rigaku, Japan) using CuK_α radiation with a wavelength, $\lambda = 1{\cdot}5418$ Å.

Table 1. Process parameters for the spray deposition of SnO_2 thin films.

Spray parameters		Annealing temperature (°C)
Constant parameters	Values	
Concentration of solution	0·075 M	550
Substrate temperature	350°C	750
Distance between spray nozzle and substrate	25 cm	
Spray rate	5 mL/min.	950
Carrier gas	Air	

The average grain size of tin oxide thin film samples were calculated by using the Scherrer equation (Cullity 1956):

$$D = 0{\cdot}9\lambda/\beta\cos\theta, \quad (3)$$

where D is the average grain size, λ=1·542 Å X-ray wavelength), and β the peak FWHM and θ the diffraction peak position. The microstructures of the films were analysed using a scanning electron microscope [SEM model JEOL 2300 Japan]. The optical absorbances of the films were measured using UV-visible-2450 spectrophotometer (Shimadzu) in the wavelength range 200–700 nm at room temperature.

2.6 *Details of gas sensing system*

The 'static gas sensing system' (Jain and Patil 2006, 2007; Thosare *et al* 2007) had been employed for testing of the films to gases. The heater was placed on a base plate to heat the sample under test up to required operating temperature. Using a syringe, a measured quantity of gas was introduced inside the static system. For the measurement of sensitivity and response and recovery times, a fixed voltage of 5 V was applied across the film. The corresponding current was measured using a picoammeter. Film response to a particular gas was studied by introducing the gas of known concentration into the glass dome and recording current as a function of time till steady state was reached. Air was allowed to pass into the glass dome after every H_2S gas exposure.

3. Results and discussion

3.1 *Structural properties of films*

Many studies on the effect of annealing temperature on film characteristics have been reported (Beshkov *et al* 1993; Wang *et al* 2006). Generally with an increase in annealing temperature, structure of the film changes from amorphous to crystalline and grain growth occurs with increase in mobility with temperature. The XRD patterns of films deposited on alumina substrate annealed with different temperatures are shown in figure 3. Films annealed at 550°C shows very small peaks indicating their predominantly amorphous nature. As the annealing temperature is increased, structural evolution is found to occur yielding polycrystalline films, characterized by an increase in intensity of peaks. The intensity of peaks is seen to increase indicating an improvement in crystallinity with annealing temperature. The (110), (101), (200) and (002) peaks match well with the standard data (JCPDS card 77-0452). All the peaks correspond to the tetragonal phase. Films on alumina substrate are seen to have preferred orientation along (022) and (002) planes. The peaks (*) marked are attributed to alumina. Similar reports of increase in crystallinity with different annealing temperatures, can be seen in literature (Shanthi *et al* 1999; Senguttuvan and Malhotra 1996). Average mean grain sizes, as inferred from XRD patterns using Scherrer method are listed in table 2.

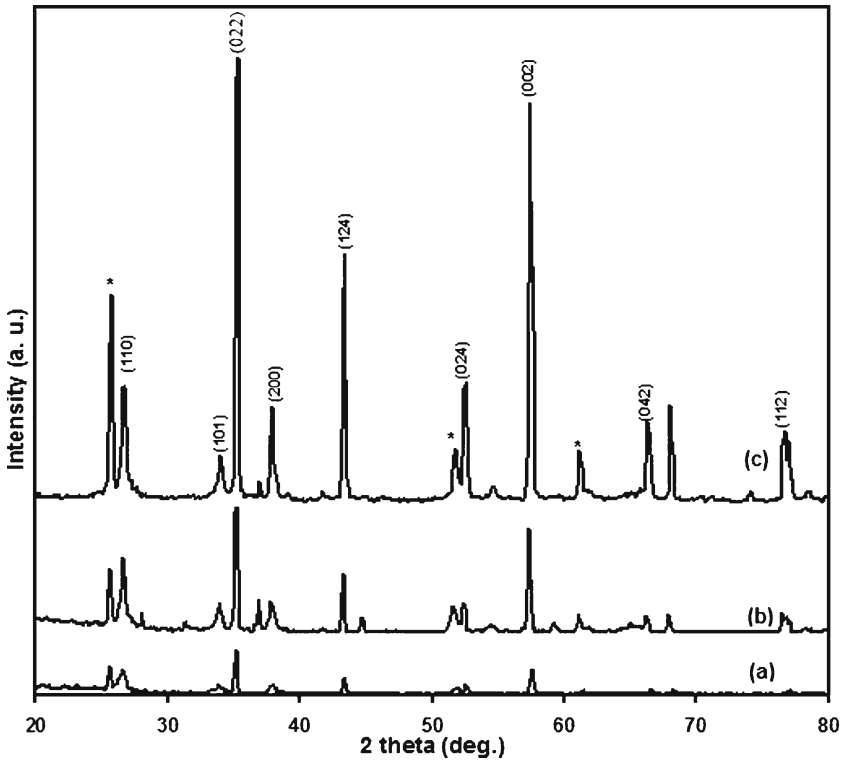

Figure 3. XRD patterns of SnO_2 thin films annealed at (**a**) 550 °C, (**b**) 750 °C and (**c**) 950 °C.

Table 2. Variation of grain size and bandgap energy with annealing temperature.

Annealing temperature (°C)	Average grain size from XRD (nm)	Average particle size from SEM (nm)	Bandgap energy (eV)
550	40·0	56·1	3·62
750	43·2	58·0	3·53
950	56·1	68·3	3·50

3.2 *Surface morphology of films*

Figure 4 consists of SEM images representing surface morphology of the SnO_2 thin films with different annealing temperatures. It is seen that the microstructure of these films are quite similar except for a small increase in particle size. The average particle size obtained from SEM images are 56·1–68·3 nm. It is found that the SnO_2 films have relatively smooth morphology (Patil *et al* 2003). The SEM images reveal increase of particle size with increasing annealing temperature, up to an approximate average particle size of 69·3 nm at 950°C. However, as determined from XRD data, the average grain size ranged from 40–56·1 nm, which was substantially smaller than the 56·1–68·3 nm dimensions of grains observed in SEM.

3.3 *Optical properties*

Absorption spectra as a function of annealing temperature for SnO_2 thin films are shown in figure 5. The absorption at higher wavelengths in the visible region is low and at wavelength, 350–380 nm, an intense absorption can be seen. Further, absorption increases as annealing temperature rises from 550–950°C.

The value of absorption coefficient (α) is of the order of 10^4 cm^{-1}. Absorption coefficient decreases with increase in annealing temperature. The bandgap of the films corresponding to annealing temperature, 550–950°C was calculated by plotting $(\alpha h\nu)^2$ vs $h\nu$ using the relation,

$$\alpha h\nu = A\left(h\nu - E_g\right)^n, \tag{4}$$

where α is absorption coefficient, A a constant, E_g the optical bandgap energy, $h\nu$ the photon energy and n a constant. The value of n is 1/2 or 2 depending on presence of the allowed direct and indirect transitions. Figure 6 shows the plots of $(\alpha h\nu)^2$ vs $h\nu$ for films at different annealing temperatures. The nature of the plots suggests direct interband transition. The bandgap is determined by extrapolating the straight line portion of the plot to the energy axis. The intercept on energy axis gives the value of bandgap energy for all the samples and it decreased from 3·62–3·5 eV by increasing the annealing temperature from 550–950°C. It is reported (Nagasawa and Shionoya 1971; Melsheimer and Ziegler 1985) that the bandgap energies for polycrystalline tin oxide were 3·35–3·3 eV and 3·9–3·5 eV, respectively. Also similar results are given in the literature for spray deposited SnO_2 thin films (Shanthi *et al* 1980; Chopra *et al* 1983; Asu and Subramaniam 1990; Patil *et al* 2003).

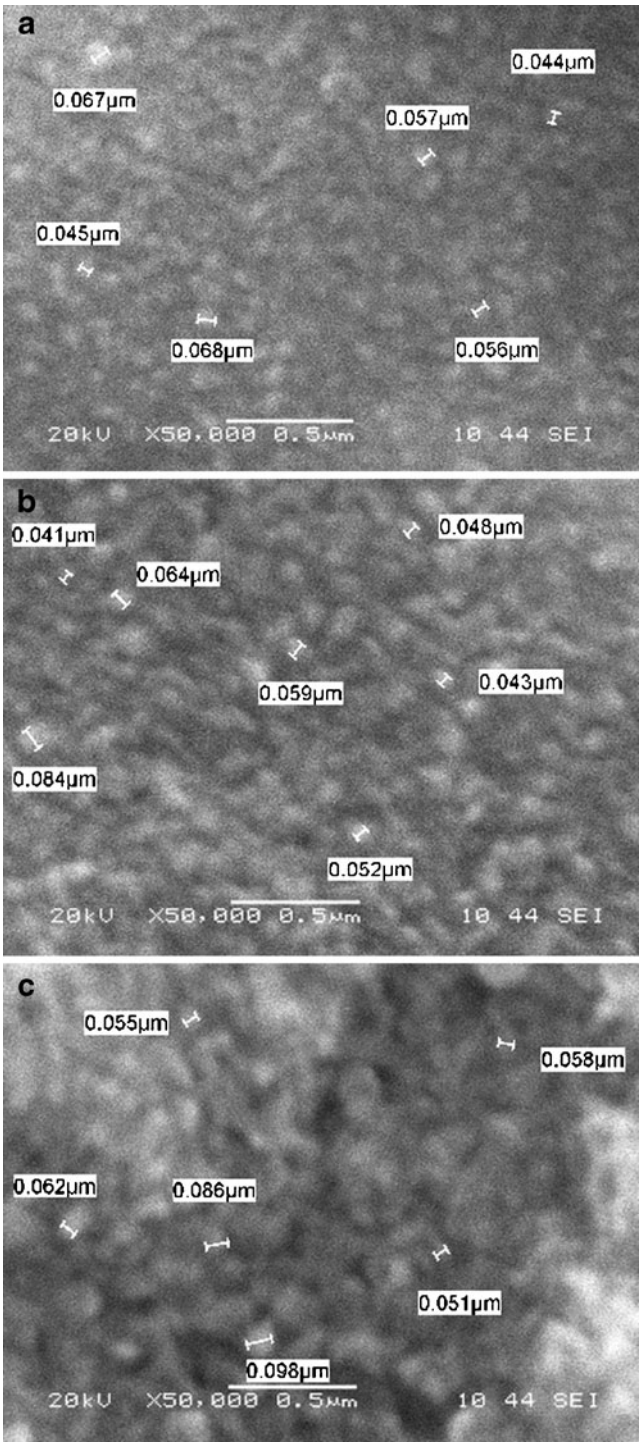

Figure 4. SEM photographs at annealing temperatures (**a**) 550°C, (**b**) 750°C and (**c**) 950°C.

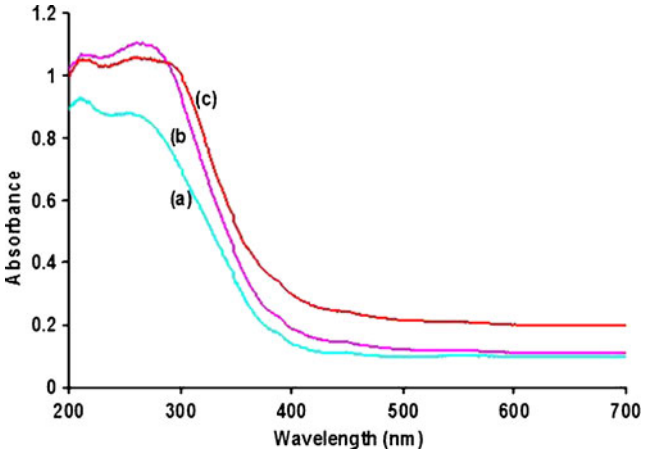

Figure 5. Variation of absorbance with wavelength (λ), nm, for annealing temperatures (**a**) 550°C, (**b**) 750°C and (**c**) 950°C.

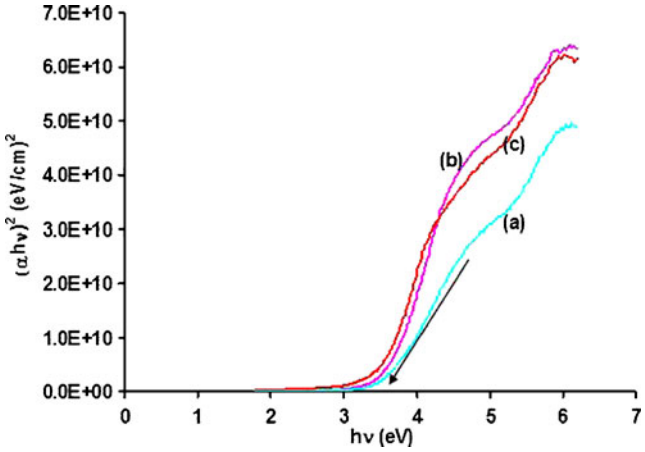

Figure 6. Plot of $(\alpha h\nu)^2$ vs photon energy $(h\nu)$ for the annealing temperatures (**a**) 550°C, (**b**) 750°C and (**c**) 950°C.

3.4 *Gas sensing properties of SnO_2 thin films*

3.4a *Basic gas sensing characteristics*: The basic gas sensing characteristics of the SnO_2 thin films were investigated as a function of operating temperature and test gas concentration. In the present studies the films were characterized by various parameters such as sensitivity, selectivity and response and recovery time.

- The sensitivity (S) is defined as $S = (R_a - R_g)/R_g$, where R_g is the resistance in presence of test gas and R_a the film resistance in dry air, measured at respective temperatures. A positive value of S implies film resistance decreases on gas exposure and *vice versa*.
- The selectivity or specificity of a sensor towards an analysing gas is expressed in terms of dimension that compares the concentration of the corresponding interfering gas that produces the same sensor signal. This factor (Aswal and Gupta 2007) is obtained by

$$\text{Selectivity} = (\text{sensitivity of sensor for interfering gas}) / (\text{sensitivity towards desired gas}).$$

- The response time is the time interval over which resistance attains a fixed percentage (usually 90%) of final value when the sensor is exposed to full scale concentration of the gas. A small value of response time is indicative of a good sensor.
- The recovery time is the time interval over which resistance reduces to 10% of the saturation value when the sensor is exposed to full scale concentration of the gas and then placed in clean air. A good sensor should have a small recovery time so that sensor can be used again and again.

3.4b *Sensitivity of SnO_2 films to H_2S with operating temperature*: The preparation of SnO_2 gas sensors usually involves annealing at a high temperature of 550–950°C (Nayral *et al* 2000; Safonova *et al* 2000; Teeramongkonrasmee and Sriyudthsak 2000; Saha *et al* 2001; Ivanoc *et al* 2004; Kotsikau *et al* 2004; Wei *et al* 2004). For comparison, the H_2S sensing properties of the SnO_2 films at different annealing temperatures were also studied under identical experimental conditions. The annealing temperature is an important parameter for gas sensing materials and in designing of sensors. The sensing materials have to be annealed at various temperatures to achieve crystallization and structural evolution. A sufficient degree of crystallinity is required to attain the desired electronic properties necessary for gas sensor application. The dependence of the sensitivity of the prepared SnO_2 to 80 ppm of H_2S at annealing temperatures of 550°C, 750°C and 950°C on the operating temperature is shown in figure 7. The sensitivity is found to be maximum when the annealing temperature was 950°C. The annealing in air renders more oxygen vacancy generation, which enhances the gas sensitivity. It is observed that the sensitivity increases from 50–100°C and then decreases with further increase in the operating temperature. It showed maximum sensitivity of 23·4, 39 and 96 to 80 ppm of H_2S at annealing temperatures 550°C, 750°C and 950°C, respectively.

3.4c *Variation in sensitivity with H_2S gas concentration*: The dependence of sensitivity of SnO_2 on the H_2S concentration at an operating temperature of 100°C is shown in figure 8. It is observed that the sensitivity increases linearly as the H_2S concentration increases from 10–80 ppm and then decreases with further increase in the H_2S concentration. The linear relationship between the sensitivity and the H_2S concentration at low concentrations may be attributed to the availability of sufficient number of sensing sites on the film to act upon the H_2S. The low gas concentration implies a lower

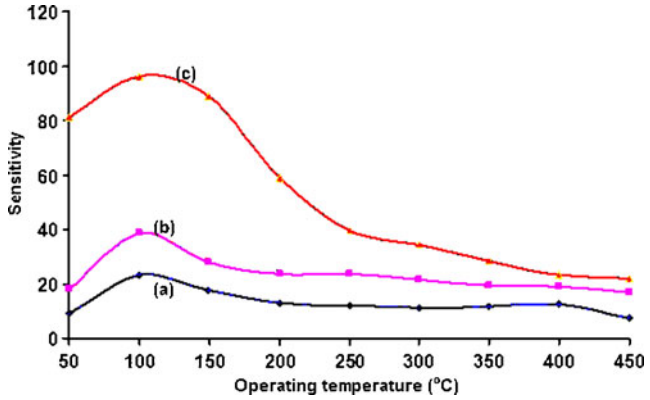

Figure 7. Effect of annealing temperature on the sensitivity of SnO_2 thin films at (**a**) 550°C, (**b**) 750°C and (**c**) 950°C to 80 ppm of H_2S gas.

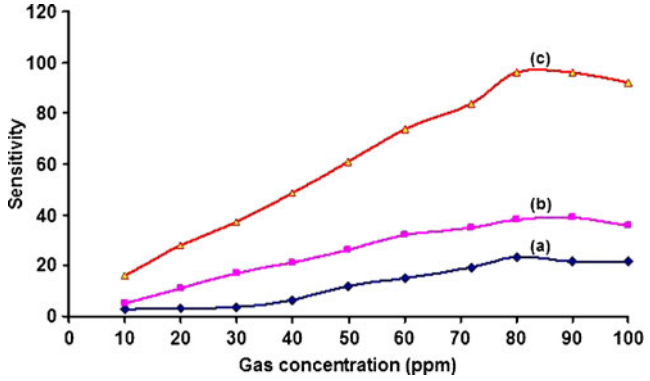

Figure 8. Dependence of the sensitivity of the SnO_2 on H_2S concentration at 100°C.

surface coverage of gas molecules, resulting into lower surface reaction between the surface adsorbed oxygen species and the gas molecules. The increase in the gas concentration increases the surface reaction due to a large surface coverage. Further increase in the surface reaction will be gradual when saturation of the surface coverage of gas molecules is reached. Thus, the maximum sensitivity was obtained at an operating temperature of 100°C for the exposure of 80 ppm of H_2S. The SnO_2 is able to detect up to 10 ppm for H_2S with reasonable sensitivity at an operating temperature of 100°C. The linearity of the sensitivity in the low H_2S concentration range (10–80 ppm) suggests that the SnO_2 can be reliably used to monitor the concentration of H_2S over this range.

3.4d *Selectivity of SnO_2 thin films for various gases*: It is observed from figure 9 that the SnO_2 thin films gives maximum sensitivity to H_2S (80 ppm) at 100°C. The films showed highest selectivity for H_2S against all other tested gases: NH_3, LPG, Cl_2, CO, CO_2, O_2, H_2 and ethanol. The selectivity also increases with annealing temperature.

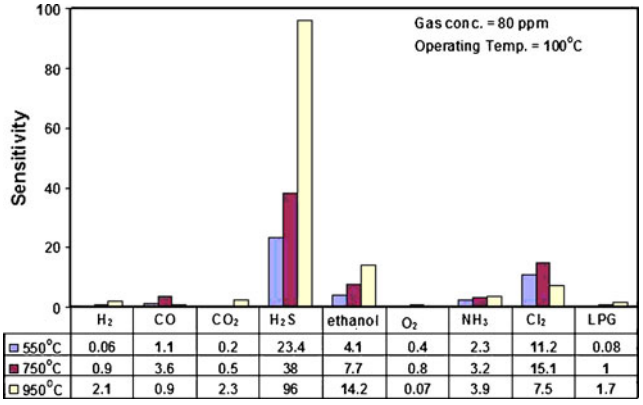

Figure 9. Selectivity of SnO_2 thin films for various gases.

3.4e *Response and recovery times*: The response and recovery of the SnO_2 film annealed at 950°C are shown in figure 10. The response was quick (∼32 s) even to a trace amount (80 ppm) of H_2S gas, while the recovery was fast (∼88 s). The quick response may be due to faster oxidation of gas. The negligible quantity of the surface reaction product and its high volatility explains its quick response and fast recovery to its initial chemical status. These results indicate that the SnO_2 prepared by spray pyrolysis method is a suitable material for the fabrication of the H_2S sensor. A number of experiments have been carried out to measure the sensitivity as a function of the operating temperature. All the time the sensitivity of the sensor element has approximately constant values, indicating the repeatability of the sensor.

3.4f *Gas sensing mechanism*: The gas sensing mechanism belongs to the surface controlled type (Jain *et al* 2007a,b) which is based on the change of the electrical conductance of the semiconducting material upon exposure to H_2S vapours. The gas sensitivity is a function of grain size, surface state and oxygen adsorption (Rothschild and Komen 2004). The surface area generally provides more adsorption–desorption sites and thus higher sensitivity. The H_2S sensing mechanism is based on the change in conductance of SnO_2 thin film, which is controlled by H_2S species and the amount of chemisorbed oxygen on the surface. It is known that atmospheric oxygen molecules are adsorbed on the surface of semiconductor oxides in the form of O_2^-, O^- or O^{2-}. The reaction kinematics may be explained by the following reactions:

$$O_2\,(\text{gas}) + e^- \rightarrow O_2\,(\text{ads})^-\,, \tag{5}$$

$$O_2\,(\text{gas})^- + e^- \rightarrow 2O\,(\text{ads})^-\,. \tag{6}$$

The presence of chemically adsorbed oxygen could cause electron depletion in the thin film surface and building up of Schottky surface barrier; consequently, the electrical conductance of thin film decreased to a minimum. The SnO_2

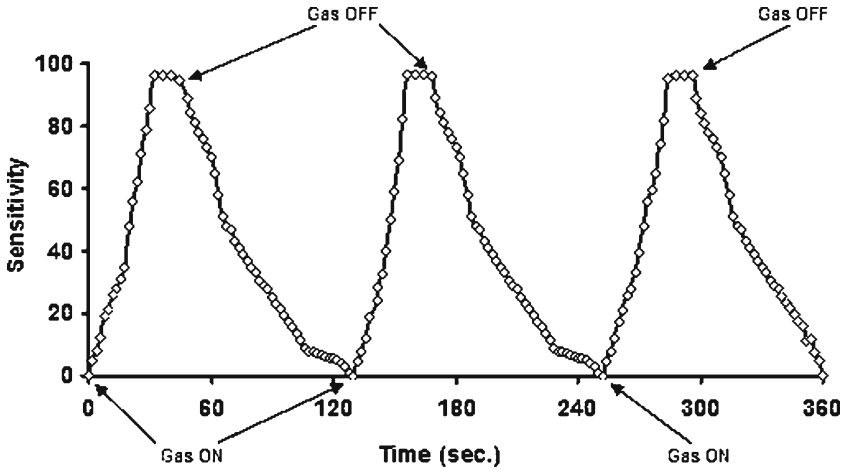

Figure 10. Response and recovery of the SnO_2 film.

thin film interacts with oxygen by transferring the electron from the conduction band to adsorbed oxygen atoms. The response to H_2S can be explained as a reaction of gas with the $O_2(ads)^-$.

$$H_2S + 3O\,(ads)^- \rightarrow H_2O\,(g) + SO_2\,(g) + 3e^-. \qquad (7)$$

With this reaction, many electrons could be released to thin film surface. This could make the Schottky surface barrier decrease, with the depletion layer thinner; consequently, the electrical conductance of the thin film increases. More gas would be adsorbed by the thin film surface; consequently, the gas sensitivity was enhanced. Increase in operating temperature causes oxidation of large number of H_2S molecules, thus producing very large number of electrons. Therefore, conductivity increases to a large extent. This is the reason why the gas sensitivity increases with operating temperature. However, the sensitivity decreases at higher operating temperature, as the oxygen adsorbates are desorbed from the surface of the sensor (Windichamann and Mark 1979). Also, at higher temperature, the carrier concentration increases due to intrinsic thermal excitation and the Debye length decreases. This may be one of the reasons for decreased gas sensitivity at higher temperature (Mizsei 1995).

4. Conclusions

The SnO_2 films were synthesized by spray pyrolysis method and the H_2S sensing properties of the SnO_2 were investigated. The following conclusions were drawn from the present investigation:

(I) We have successfully prepared SnO_2 films by spray pyrolysis method using $SnCl_2{\cdot}2H_2O$. The resulting SnO_2 films was characterized by XRD measurements and SEM.

(II) As annealing temperature increases grain size increases.

(III) The bandgap values obtained from the absorption spectra was found to be 3·62–3·5 eV.

(IV) The maximum sensitivity was obtained at an operating temperature of 100°C for the exposure of 80 ppm of H_2S.

(V) The results of the H_2S sensing studies reveal that the SnO_2 films prepared by spray pyrolysis method are a suitable material for the fabrication of the H_2S sensor.

Acknowledgements

The authors are thankful to the University Grants Commission, New Delhi and BCUD, University of Pune, Pune, for providing financial support. Thanks to Principal, Arts, Commerce and Science College, Nandgaon, for providing laboratory facilities for this work. Authors are grateful to Dr L A Patil, Nanomaterials Research Lab., Pratap College, Amalner and Dr D P Amalnerkar, Director, C-MET, Pune, for their valuable cooperation rendered for characterizations of the material.

References

Aoki A and Sasakura H 1970 *J. Appl. Phys.* **9** 582

Asu V V and Subramaniam A 1990 *Thin Solid Films* **189** 217

Aswal D K and Gupta S K 2007 *Science and technology of chemiresistor gas sensors* (New York: Nova Sci. Publishers) p.37

Baranauskas V, Santos T E A, Schreiner M A, Zhao J G, Pellegrini Mamman A and Zamitti Mammana C I 2002 *Sensor Actuat.-B. Chem.* **85** 90

Beshkov G, Kolentsov K, Yourukova L, Rachkova A and Mateeva D 1993 *Mater. Sci. Eng.* **B30** 1

Betz U, Kharrazi, Olsson M, Marthy J, Escola M F and Atamny F 2006 *Surf. Coat. Technol.* **200** 5751

Blandenet G, Court M and Lagarde Y 1981 *Thin Solid Films* **77** 81

Chatelon J P, Tenier C, Bemstein E, Berjoan R and Roger J A 1994 *Thin Solid Films* **247** 162

Chopra K L, Major S and Pandya D K 1983 *Thin Solid Films* **102** 1

Cullity B D 1956 *Elements of X-ray diffraction* (USA: Addison-Wesley Publishing Co.)

DiBattista M, Korotcenkov G, Schwank J and Brinzari V 2000 *Mater. Sci. Eng.* **B77** 33
Fukano T and Motohiro T 2004 *Sol. Energy Mater. Sol. Cells* **82** 567
Gurav A S, Kodas T T, Joutsensaari J, Kauppinen E I and Zilliacus R 1995 *J. Mater. Res.* **10** 1644
Hartnagel H L 1995 *Semiconducting transparent thin films* (Bristol and Philadelphia: Institute of Physics Publishing)
Ivanoc P, Llobet E, Vilanova X, Brezmes J, Hubalek J and Corrig X 2004 *Sensor Actuat. B-Chem.* **99** 201
Jain G H and Patil L A 2006 *Bull. Mater. Sci.* **29** 403
Jain G H and Patil L A 2007 *Sensor Actuat.-B: Chem.* **123** 246
Jain G H, Patil L A and Gaikwad V B 2007a *Sensor Actuat. B-Chem.* **122** 606
Jain G H, Patil L A, Patil P P, Mulik U P and Patil K R 2007b *Bull. Mater. Sci.* **30** 9
Khadayate R S, Waghulde R B, Wankhede M G, Sali J V and Patil P P 2007 *Bull. Mater. Sci.* **30** 129
Keshavraja A, Ramaswami A V and Vijayamohanan K 1995 *Sensor Actuator* **B23** 75
Kodas T T and Hampden-Smith M J 1999 *Aerosol processing of materials* (New York: Wiley-Vch) p. 421
Korotcenkov G, Macsanov V, Tolstoy V, Brinzari V, Schwank J and Faglia G 2003 *Sensor Actuat.-B: Chem.* **96** 602
Korotcenkov G, Cornet A, Rossinyol E, Arbiol J, Brinzar V and Blinov V 2005 *Thin Solid Films* **471** 310
Kotsikau D, Ivanovskaya M, Orlik D and Falasconi M 2004 *Sensor Actuat. B-Chem.* **101** 199
Liu H, Gong S P, Hu Y X, Liu J Q and Zhou D X 2009 *Sensor Actuat.* **B140** 190
Melsheimer J and Ziegler D 1985 *Thin Solid Films* **129** 35
Mizsei J 1995 *Sensor Actuat.* **B23** 173
Mohammadi M, Solemani E and Mansorhaseini M 2005 *Mater. Res. Bull.* **40** 1303
Nagasawa M and Shionoya S 1971 *J. Phys. Soc. Jpn* **30** 1118
Nayral C, Viala E, Colliere V, Fau P, Senocq F, Maisonnat A and Chaudret B 2000 *Surf. Sci.* **164** 19
Oreal B, Lavrencic-Stangar U, Cmjak-Olel, Bukovea P and Kosec M 1994 *J. Non-Cryst. Solids* **167** 272
Paraguay F, Estrada D W, Acosta L D R, Andradeb N E and Miki-Yoshida M 1999 *Thin Solid Films* **350** 192
Patil P S 1999 *Mater. Chem. Phys.* **59** 185
Patil P S, Kawa R K, Sadale S B and Chigare P S 2003 *Thin Solid Films* **437** 34
Randhawa H S, Mathews M D and Bunshah R F 1981 *Thin Solid Films* **83** 267
Rothschild A and Komen Y 2004 *J. Appl. Phys.* **95** 6374
Safonova O V, Rumyantseva M N, Ryabova L I, Labeau M, Delabouglise G and Gaskov A M 2000 *Mater. Sci. Eng. B Solid State Mater. Adv. Technol.* **85** 43
Saha M, Banerjee A, Halder A K, Mondal J, Sen A and Maiti H S 2001 *Sensor Actuat. B-Chem.* **79** 192
Sears W M and Gee M A 1998 *Thin Solid Films* **165** 265
Seiyama T, Kato A and Nagatani M 1962 *Anal. Chem.* **34** 1502
Senguttuvan T D and Malhotra L K 1996 *Thin Solid Films* **289** 22
Shanthi E, Banerjee A and Chopra K L 1980 *J. Appl. Phys.* **51** 6243
Shanthi S, Subramanian C and Ramasamy P 1999 *J. Cryst. Growth* **197** 858
Taguchi N 1962 Japanese Patent Application
Teeramongkonrasmee A and Sriyudthsak M 2000 *Sensor Actuat. B-Chem.* **66** 256
Thosare S R, Bari R H, Jain G H and Patil L A 2007 *Advanced materials and applications: Proc. ICAMA-2007*, *Shivaji University, Kolhapur*
Vossen J L and Poliniak E S 1972 *Thin Solid Films* **13** 281
Vuong D D, Sakai G, Shimanoe K and Yamazoe N 2005 *Sensor Actuat. B-Chem.* **105** 437
Wang M, Eui J K, Jin S C, Eun W S, Sung H H, Ka E L and Park C 2006 *Phys. Status Solidi* **203** 2418
Wei B Y, Hsu M C, Su P G, Lin H M, Wu R J and Lai H J 2004 *Sensor Actuat. B-Chem.* **101** 81
Windichamann H and Mark P 1979 *J. Electrochem. Soc.* **126** 627